

RMOPP: Robust Multi-Objective Post-Processing for Effective Object Detection

Mayuresh Savargaonkar Abdallah Chehade
 Department of Industrial and Manufacturing Systems Engineering
 University of Michigan-Dearborn

Samir Rawashdeh
 Department of Electrical and Computer Engineering
 University of Michigan-Dearborn

mayuresh@umich.edu achehade@umich.edu srawa@umich.edu

Abstract

Over the last few decades, many architectures have been developed that harness the power of neural networks to detect objects in near real-time. Training such systems requires substantial time across multiple GPUs and massive labeled training datasets. Although the goal of these systems is generalizability, they are often impractical in real-life applications due to flexibility, robustness, or speed issues. This paper proposes RMOPP: A robust multi-objective post-processing algorithm to boost the performance of fast pre-trained object detectors with a negligible impact on their speed. Specifically, RMOPP is a statistically driven, post-processing algorithm that allows for simultaneous optimization of precision and recall. A unique feature of RMOPP is the Pareto frontier that identifies dominant possible post-processed detectors to optimize for both precision and recall. RMOPP explores the full potential of a pre-trained object detector and is deployable for near real-time predictions. We also provide a compelling test case on YOLOv2 using the MS-COCO dataset.

1. Introduction

Object detectors and vision systems have greatly advanced in the last few years. The evolution of deep neural networks has unlocked new potential in complex fields such as capacity estimations of Li-ion battery cells [36, 33, 6] and Remaining-Useful-Life (RUL) predictions [35, 4, 5]. The field of object detection and classification is another significant beneficiary of this especially due to the advancements in Convolutional Neural Networks (CNNs). In this paper, we refer to the broader task of detection and classification simply as object detection. Deep convolution neural net-

works commonly outperform traditional methods such as ones using Support Vector Machines (SVMs) or regression techniques [24]. CNNs are typically either run as a single-stage detector or a two-stage detector. More details on state-of-art detectors are provided in the literature review.

Research today mainly focuses on building object detection systems that offer a reasonable trade-off between speed and accuracy. For improved accuracy, two-stage detectors including ensemble neural networks like PA Net [25] are shown to perform well in competitions like PASCAL VOC [27], MS-COCO [23], and ImageNet [7]. Although such systems provide competition winning performances, they sacrifice speed and are not currently suitable for deployment in real-time systems. For improved latency, single-stage detectors like the YOLO series algorithms: YOLOv1 [30], YOLOv2 [31], and YOLOv3 [10] are shown to be faster than two-stage detectors. Although single-stage detectors are extremely fast, they often fail to reach the same level of robustness as the two-stage detectors [24]. Robustness here is defined as the ability of an object detection pipeline to successfully handle perturbations. Single-stage detectors' limitations are often associated with localization errors and the identification of false positives [29]. This makes them less suitable for critical applications that require high robustness.

Practically, for many real-life applications like object detection in autonomous vehicles in Figure 1, both, detection of an object and speed are deemed extremely important. A failure in detection, as well as a slow detection, can result in a fatal crash. Further, these object detection pipelines are often hard-wired to achieve high precision at lower recall or higher recall at lower precision to achieve competition winning performances. Therefore, there is an essential need for a customizable and low-latency object detection pipeline with a robust post-processing method that can pro-

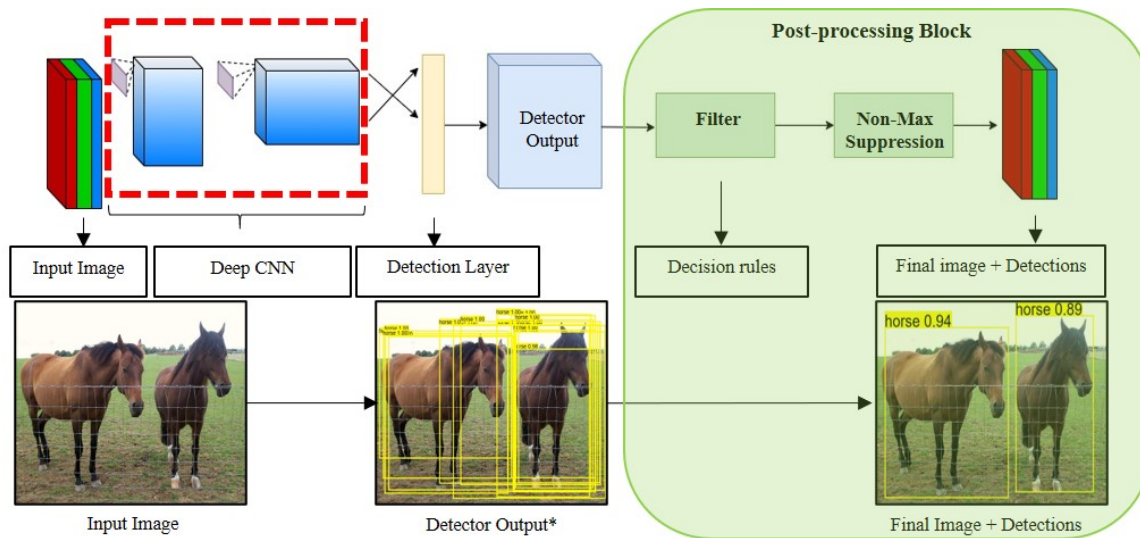


Figure 2: Object detection pipeline using a single-stage detector. *Detector output is cleaned for visualization purposes.

periments with ATSS, Zhang *et al.* [43] show that definitions of positive and negative annotations help bridge traditional gaps between anchor-free and anchor-based methods.

End-to-end object detection is another branch of single-stage detectors that try to improve performance by eliminating the post-processing stages such as NMS (Non-Maximal Suppression). DETR [3] is the first such detector that is capable of performing end-to-end object detection. OneNet [38] is another recent end-to-end object detector that achieves state-of-art while running at real-time speeds. While end-to-end object detectors achieve unparalleled performances in speed and accuracy, they lack customizability offered by post-processing stages. Customizations require re-training using several GPUs and hours of complex training paradigms often unavailable to the common user. The importance of this subject is also touched upon by J. Huang *et al.* [18], although they focus more on exploiting the aspect of speed and accuracy trade-offs for developing a better detector. While investigating the effect of speed on accuracy for a wide range of detectors, they show that the single-stage detectors based on the ResNet 101 backbone perform equally well when compared to R-FCN [18] and Faster RCNN on the same backbone for large object detection on the MS-COCO dataset.

2.2. Post-Processing Algorithms: State-of-Art

Most existing object detectors start with outputting four bounding box co-ordinates, a score, and the class associated with each one of the detections. The commonly used ‘score’ function for detection is the product of the probability of the most probable class bounded in an identified detection and the confidence of having an object inside the

detected box. Next, detections with low scores are filtered assuming that lower scores represent poorly identified or classified objects. Once the detections are filtered, NMS is applied with a pre-defined NMS threshold (η) [1]. NMS is the process of identifying detections with the Intersection over Union (IoU) greater than the NMS threshold (η) and then eliminating those with lower ‘scores’. The NMS process is effective in eliminating redundant detections.

A significant improvement in post-processing comes as the ‘Soft-NMS’ replacing the traditional greedy NMS [1]. This work has shown to be of little use in the case of complex datasets like the PASCAL VOC and MS-COCO [1]. To propose a suitable improvement over the ‘Soft-NMS’, He *et al.* [15] introduced the ‘Softer-NMS’ which decays the bounding box scores using a continuous function thus achieving better results. Relation networks [17] and Learning NMS [16] are amongst some other types of works that try to improve upon the traditional NMS by designing and training a sub-network to analyze complex object-object correlations. While works such as Fitness NMS [41] try to integrate localization information into ranking scores, LTR [39] is another sub-network that improves on suppression ranking via learning procedures. NMS based post-processing works show promising performance gains and thus help build confidence that effective post-processing is key in any suitable object detection pipeline. A summary of a common single-stage object detection pipeline is shown in Figure 2.

Although there exist post-processing algorithms, they often fail to explicitly acknowledge the fact that there may exist multiple recalls at the same precision and vice-versa. Thus, they fail to explore the full potential of an object de-

Probability of most probable class \ Probability of existence of bounding box	Low	High
	Block I Block III	Block II Block IV

Table 1: The blocks in ‘**bold**’ show where the existing post-processing algorithms are effective.

tection pipeline which results in sub-optimal detection performance. RMOPP thus uses the concepts of Pareto frontier which identifies a set of dominant post-processing hyper-parameters that optimize both precision and recall simultaneously. More details are provided in Section 4.

3. Proposed Algorithm: RMOPP

Existing post-processing algorithms rely on a single data-driven ‘score’ metric that is not statistically intuitive. Several assumptions are made when filtering detections by scores and NMS using pre-defined post-processing hyper-parameters and thresholds. These values are usually chosen on an empirical basis, user’s experience, or by using a trial-and-error method. Hereafter, we will focus on the most common ‘score’ function for existing post-processing algorithms that is defined by the product of the probability of the most probable class bounded in an identified detection and the confidence of having an object inside the detected bounding box.

With this definition of the score function, Table 1 summarizes the output of commonly used object detectors. Block I comprise detections with poor scores that are typically filtered out. Block IV comprises of detections with high scores that are typically retained. Block II and III comprise of risky detections with intermediate scores. The existing post-processing algorithms are susceptible to poor performance for detections in Block II and III that have intermediate level scores. Many of those detections are (i) mistakenly filtered out (a large number of false negatives) thus achieving a lower than ideal recall or, (ii) poor detections are retained (a large number of false positives) thus achieving a lower than ideal precision. To address this limitation, we introduce RMOPP: A robust multi-objective, post-processing algorithm that allows simultaneous and optimized tuning of recall and precision.

3.1. Proposed Post-Processing Algorithm

Let (X^c) be the binary random variable associated with the existence of some bounding box (c) with probability (P_c) . Let (X_i^c) be the binary random variable

indicating that the object in the bounding box (c) belongs to a class (i) with probability (P_i^c) . Under the assumptions that $X^c \sim Ber(P_c)$ and the collection $\{X_1^c, \dots, X_i^c, \dots, X_N^c\} \sim MultiNom(P_i^c, \dots, P_N^c, 1)$,

$$E[X^c] = P(X^c = 1) = P_c \quad (1)$$

$$E[X_i^c] = P(X_i^c = 1) = P_i^c \quad (2)$$

$$\sum_{i=1}^N P_i^c = 1 \quad (3)$$

To simplify the mathematical notations, let (Z_i^c) be the ordered statistic of (X_i^c) such that $P(Z_i^c = 1) \times P(Z_j^c = 1) \forall j > i$. Under this notation, $P(Z_i^c = 1)$ is the probability of the most probable class for the detection bounded in the box (c) and the existing post-processing technique is expressed as,

$$s^c = P(Z_1^c = 1) \times P(X^c = 1) \leq \gamma \quad (4)$$

where the detection in the box (c) is filtered out if its score (s^c) is less than a pre-defined threshold (γ) as stated in Equation 4. The threshold (γ) is often chosen based on empirical analysis, user experience, or by limited trials. Extensions of the of Equation 4 exist where the score is defined as $\max_i P(X_i^c = 1)$ or as $\max_i P(X^c = 1)$. It should be noted that if the object detector does not output the confidence $P(X^c = 1)$, then $P(X^c = 1)$ is set to 1 for all detections.

Note that during training, object detectors aim to minimize the population cross-entropy over the training dataset. Therefore, it is natural to design a post-processing algorithm that shares similar merit to the training procedure. Specifically, we consider thresholding over the log-likelihood ratios of the most probable class to all other classes for every bounding box. This brings us to our first proposition.

Proposition I: The log-likelihood ratios between the top class and the remaining classes of a bounding box (c) are sufficient to quantify the classification accuracy of the object in the bounding box (c) .

Proposition I is inspired by the likelihood ratio test and the theory of statistical hypothesis testing, which shows that every bounding box (c) must satisfy $\left(\frac{P(Z_1^c=1)}{P(Z_k^c=1)}\right) \geq \gamma_1, \forall k > 1$.

Lemma I: Given the definition that (Z_i^c) is the ordered statistic of (X_i^c) such that $P(Z_i^c = 1) \times P(Z_j^c = 1) \forall j > i$. Then, $\left(\frac{P(Z_1^c=1)}{P(Z_2^c=1)}\right) \geq \gamma_1$ for any bounding box (c) guarantees $\left(\frac{P(Z_1^c=1)}{P(Z_k^c=1)}\right) \geq \gamma_1, \forall k > 1$. From Lemma I and Proposition I, we identify our first score metric to be $\left(\frac{P(Z_1^c=1)}{P(Z_2^c=1)}\right)$

and its user-defined threshold to be (γ_1) . Therefore, any detected box (c) must satisfy Equation 5 or it will be removed for poorly classifying its bounded object.

$$\left(\frac{P(Z_1^c = 1)}{P(Z_2^c = 1)}\right) \geq \gamma_1, \forall c \quad (5)$$

While the classification task is critical in object detection, the bounding box detection is also an important task. Proposition I guarantees a good classification but it does not guarantee a good bounding box detection. This brings us to Proposition II.

Proposition II: An effective object detector must show a relatively similar classification and detection performance which can be quantified by the log-likelihood ratio of detection to classification for any bounding box (c), $\left(\frac{P(X^c=1)}{P(Z_1^c=1)}\right)$, $\forall k > 1$.

Proposition II suggests that a detected bounding box truly bounds an object if $\left(\frac{P(X^c=1)}{P(Z_1^c=1)}\right)$, $\forall k > 1$, is large enough. It should be noted here that there exists a cross-correlation between Propositions I and II, where Proposition II mainly focuses on the relative detection performance given the classification probabilities $P\{(X^c = 1)|P(Z_1^c = 1), \dots, P(Z_N^c = 1)\}$ for any detected bounding box (c), thus ensuring that the boxes are well-identified and classified.

Lemma II: Given the definition that (Z_i^c) is the ordered statistic of (X_i^c) such that $P(Z_i^c = 1) \times P(Z_j^c = 1) \forall j > i$. Then, $\left(\frac{P(X^c=1)}{P(Z_1^c=1)}\right) \geq \gamma_2$ for any bounding box (c), guarantees $\left(\frac{P(X^c=1)}{P(Z_k^c=1)}\right) \geq \gamma_2$, $\forall k > 1$. From Lemma II and Proposition II, we identify our second score metric to be $\left(\frac{P(X^c=1)}{P(Z_1^c=1)}\right)$ and its user-defined threshold to be (γ_2) . Therefore, any detected box (c) must satisfy Equation 6 or it will be considered a false detection and removed.

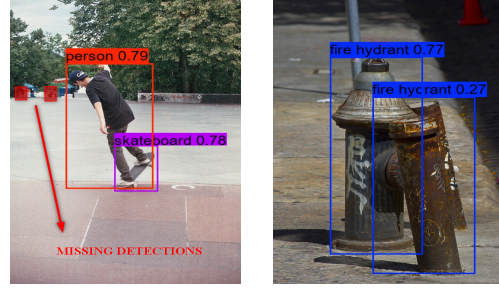
$$\left(\frac{P(X^c = 1)}{P(Z_1^c = 1)}\right) \geq \gamma_2, \forall c \quad (6)$$

Both Equations 5 and 6 summarize the proposed post-processing algorithm, where a bounding box (c) is a good detection if and only if,

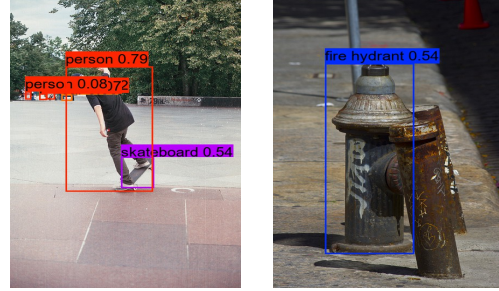
$$\left(\frac{P(Z_1^c = 1)}{P(Z_2^c = 1)}\right) \geq \gamma_1 \cap \left(\frac{P(X^c = 1)}{P(Z_1^c = 1)}\right) \geq \gamma_2, \forall c \quad (7)$$

3.2. Advantages of RMOPP

Equation 5 reduces the chances of having false positives due to poor classification. This addresses the problems with Block III in Table 1 for traditional post-processing algorithms because it filters out detections with low $\left(\frac{P(X^c=1)}{P(Z_1^c=1)}\right)$.



(a) Before using RMOPP



(b) After using RMOPP

Figure 3: (γ_1) and (γ_2) enable RMOPP to perform effective post-processing while eliminating false positives.

Note that a lower value for $\left(\frac{P(X^c=1)}{P(Z_1^c=1)}\right)$ indicates poor classification based on Lemma I and Proposition I. Thus, it is hypothesized that increasing the value (γ_1) will reduce false positives due to poor classification. Note that extreme values for (γ_1) may have a detrimental effect on true positives, thus increasing the false negatives and lowering precision and hence, should be chosen carefully. More details and results are presented in Section 4.

Further, Lemma II helps address problems due to cases following Block II in Table 1. Intuitively, $P(Z_1^c = 1)$, should only be considered when $P(X^c = 1)$ is high enough. At random detections where $P(X^c = 1)$ is low and $P(Z_1^c = 1)$ is very high, we can observe that the traditional algorithms fail as they eliminate too many true positives. Thus, it is hypothesized that a lower (γ_2) will help increasing true positives by keeping detections that were traditionally eliminated due to poor identification. The cross-correlation between (γ_1) and (γ_2) will be particularly helpful here in keeping the false positives at bay. Figure 3 shows how results improve when RMOPP is used for filtering the detections compared to the traditional algorithms.

3.3. Selecting Hyper-Parameters (γ_1) and (γ_2)

Choosing (γ_1) and (γ_2) is a non-trivial task that depends on the object detector's raw output. This is further elaborated in the case-study. Generally, decreasing both (γ_1) and (γ_2) will result in filtering out fewer detections. In ex-

Algorithm 1 Pseudocode for RMOPP

Require: $\left\{ \underset{i}{\operatorname{argmax}} X_i^c, Z_1^c, Z_2^c, X^c, b^c \right\}_{c=1}^M$
 M predictions for a given image with bbox coord b^c ;
 δ_1, δ_2 are the increments for γ_1, γ_2 ;
for $\Delta_2^L \leq \gamma_2 \leq \Delta_2^U$ **do**
 for $\Delta_1^L \leq \gamma_1 \leq \Delta_1^U$ **do**
 $I = 0^M$; an indicator if the detections satisfy Eq. 7
 for $c = 1, \dots, M$ **do**
 if $\left(\frac{P(Z_1^c=1)}{P(Z_2^c=1)} \right) \geq \gamma_1$ and $\left(\frac{P(X^c=1)}{P(Z_1^c=1)} \right) \geq \gamma_2$ **then**
 $I[c] = 1$
 end if
 end for
 if $\sum(I) \neq 0$ **then**
 apply NMS with $\text{IoU} = \eta$
 compute *Precision, Recall* and F_1
 end if
 $\gamma_1 = \gamma_1 + \delta_1$
 end for
 $\gamma_2 = \gamma_2 + \delta_2$
end for
return *Precision, Recall* and F_1 scores $\forall \gamma_1$ and γ_2

treme cases, this may result in poor precision due to extreme under-filtering. Similarly, increasing both (γ_1) and (γ_2) will result in filtering out increasing detections. In extreme cases, this may result in poor recall due to extreme over-filtering. We recommend that the user first decide on the evaluation metric of interest. The common three metrics we discuss in this paper are Precision, Recall, and F_1 score. Once decided, we apply Algorithm 1 with varying values of (γ_1) and (γ_2) to fully understand the complex correlations between the evaluation metric and (γ_1) and (γ_2) . The Pareto frontier is then identified from these values which helps optimize for recall and precision simultaneously. It is worth noting that although there may exist multiple combinations of (γ_1) and (γ_2) that result in the same precision (or recall) but different recalls (or precisions) only the dominant combinations will be identified by the Pareto frontier. More details are provided in Section 4 (Figure 4 and Figure 5). Unlike existing post-processing algorithms, RMOPP is multi-objective and hence provides the utmost flexibility in simultaneously optimizing for precision and recall.

In summary, the object detection pipeline with RMOPP performs the following steps: (1.) Take an input image and pass it through the pre-trained detector that outputs some detections, (2.) Filter these detections using Equation 7, given some values for (γ_1) and (γ_2) (3.) Perform NMS on detections from step 2 to further refine the results using NMS threshold (η) , (4.) Calculate precision, recall, and F_1 scores, (5.) Modify values of (γ_1) and (γ_2) and repeat steps

(2-5), (6.) Choose the best values of (γ_1) and (γ_2) based on preference for precision, recall, and/or F_1 scores. It should also be noted that since there is no formal specification of the NMS threshold (η) , we default it to 0.5 for all experiments unless specified otherwise.

4. Case Study: YOLOv2 using Darknet-19

While RMOPP is a suitable add-on for most of the available object detectors, we consider applying it to improve YOLOv2 in this case-study. YOLOv2 is one of the fastest existing object detectors; however, it detects many erroneous boxes and that makes it an excellent case-study for evaluating the efficacy of post-processing algorithms.

YOLOv2’s backbone is called as ‘Darknet-19’ that consists of 19 hidden convolutional layers, and it was first introduced in 2017 [31]. It is one of the fastest architecture around and performs about 5.58 billion operations per image [31]. The YOLOv2 loss function is a multi-part loss function which is a weighted sum of classification, localization, and confidence losses [30]. The ‘classification loss’ represents the loss based on the squared error of conditional class probabilities of the detected object given by the softmax layer of the detector. The ‘localization loss’ represents the loss based on the difference between coordinates of the bounding boxes for detected objects and the coordinates of bounding boxes in annotations. Note that a weighting parameter (λ_{coord}) is used to increase the contribution of localization loss in the overall loss function. ‘Confidence loss’ represents the loss concerning the objectness score for each bounding box. Since we expect more boxes for background class, to eliminate the class imbalance, another weighting parameter (λ_{noobj}) is used to down weight the contribution of confidence loss in the overall loss function when a bounding box is identified as a background object. (λ_{coord}) and (λ_{noobj}) are set to 5 and 0.5 by the Redmon *et al.* in [31].

The MS-COCO dataset used for training YOLOv2 consists of around 118,000 images with an average of 7 boxes per image and a total of 80 unique class labels [23]. For performance evaluation, we use the COCO *minival* dataset which has 5000 images that were not used in training the YOLOv2, and set the input image resolution to 544x544 for all our experiments.

4.1. Results: Precision, Recall, and F_1 score

In this case study, we use the definitions of precision, recall, and F_1 score as given in Equations 8,9 and 10. A detection is considered as a true positive if the (IoU) is greater than 0.5 with at least one ground truth annotation of the same class label. Note that if multiple objects have (IoU) more than 0.5, then only the one with the highest (IoU) is selected as a true positive while others are considered to be false positives. All unmatched objects in the list of ground

truths are considered to be false negatives. For this case-study (γ_1) is varied between 1 and 10 with increments of 0.5 and (γ_2) is varied between 0.1 and 1 with increments of 0.05. Beyond those limits, YOLOv2 showed extremely poor precisions or recalls.

$$\text{Precision} = \frac{\text{True Positives}}{\text{True Positives} + \text{False Positives}} \quad (8)$$

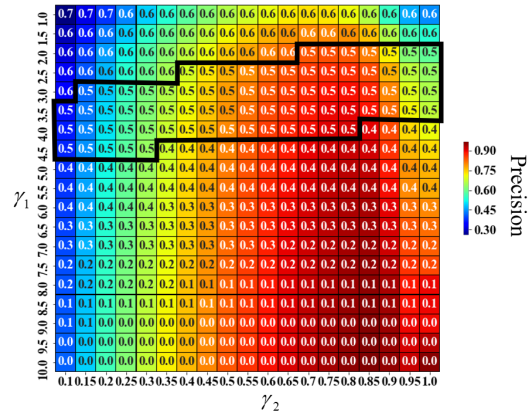
$$\text{Recall} = \frac{\text{True Positives}}{\text{True Positives} + \text{False Negatives}} \quad (9)$$

$$F_1 \text{ score} = \frac{2 \times \text{Precision} \times \text{Recall}}{\text{Precision} + \text{Recall}} \quad (10)$$

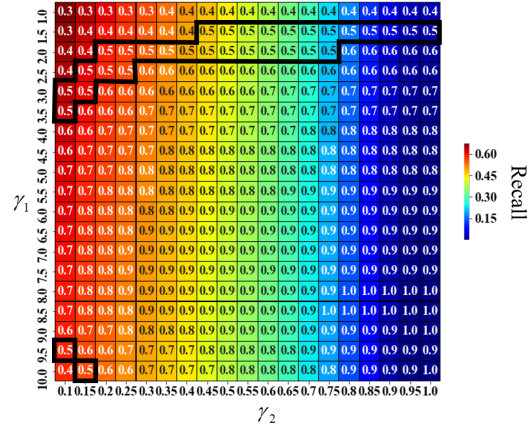
Changes in (γ_1) and (γ_2) have a significant effect on precision, recall, and F_1 scores. Essentially, (γ_1) and (γ_2) can be perceived as tuning knobs that can be used to tune the object detector for desired precision, recall, or F_1 score. In Figure 4a it is seen that as (γ_1) is increased, a smooth decrease in recall is observed with recall almost dropping to 0 for the highest values of (γ_2). Similarly, in Figure 4b it is observed that as (γ_2) is increased, precision increases almost linearly to 0.9 or more when (γ_2) is augmented from 0.1 to 1 for all values of (γ_1) above 5.5. For values of (γ_1) lower than 5.5 this increase is not so significant due to the correlation between (γ_1) and (γ_2).

When (γ_1) and (γ_2) are set to highest values, total detections drop, and a maximum precision condition (Recall \approx 0) is realized. Similarly, when (γ_1) and (γ_2) are set to lowest values, total detections rise and a maximum recall condition (Precision \approx 0) is realized. This helps build a sense of confidence which suggests that by employing finer adjustments in (γ_1) and (γ_2), we can explore the entire possible space of precision-recall offline. In this case study, multiple post-processed detectors with different (γ_1) and (γ_2) resulted in the same precision but different recall (and vice versa). The region highlighted in Figure 4a shows possible combinations of (γ_1) and (γ_2) where recall is fixed to 0.5. The regions highlighted in Figure 4b show possible combinations of (γ_1) and (γ_2) where precision is fixed to 0.5.

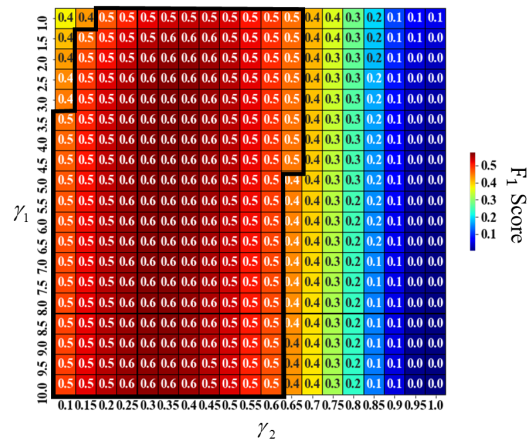
Designing a bi-objective function to simultaneously optimize precision and recall is challenging, thus, researchers have developed metrics like F_1 score to address this challenge. In Figure 4c we plot a heat map of F_1 scores in Figure 4c by varying (γ_1) and (γ_2). Although Figure 4c helps us understand the complex correlations between (γ_1), (γ_2), precision and recall, it offers limited help in selecting values of (γ_1) and (γ_2) that maximize precision at given recall and vice-versa. Thus, we plot a Pareto frontier using results obtained by varying (γ_1) and (γ_2). The Pareto frontier is plotted as a function of precision and recall in Figure 5. Here, we use the concepts of ‘Pareto Optimality’ [19] and extend them to the field of object detection for the



(a) The labels inside the figure denote recall while the color represents precision. The highlighted region encloses combinations of (γ_1) and (γ_2) where recall=0.5.



(b) The labels inside the figure denote precision while the color represents recall. The highlighted region encloses combinations of (γ_1) and (γ_2) where precision=0.5.



(c) The highlighted region encloses combinations of (γ_1) and (γ_2) where F_1 score \geq 0.5.

Figure 4: Effects of (γ_1) and (γ_2) on Precision, Recall and F_1 score.

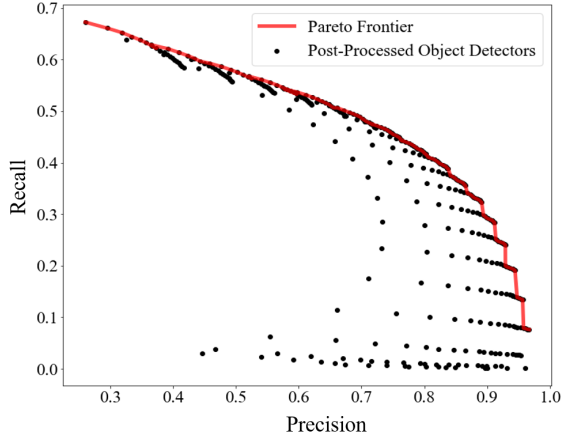


Figure 5: Pareto Frontier based on precision and recall. Here, each combination of (γ_1) and (γ_2) is a uniquely post-processed object detector and is represented by a ‘black’ dot.

first time, to the best of our knowledge. In object detection, ‘Pareto Optimality’ is defined as a condition where no improvements can be made to either precision or recall without some sacrifice in another. Such combinations of (γ_1) and (γ_2) which achieve an optimal trade-off between precision and recall are called ‘Pareto Optimal’ points. A set of such Pareto optimal points is called as ‘Pareto Frontier’. Pareto optimal points are said to dominate non-optimal points because there exists no other combination of (γ_1) and (γ_2) which achieves a better precision (or recall) at a higher recall (or precision). Figure 5 shows a plot of each unique combination of (γ_1) and (γ_2) and their associated precision and recall as a solid ‘black’ dot. A Pareto frontier is highlighted in ‘red’ in this figure which helps choose the best possible combinations of (γ_1) and (γ_2) that maximize precision at given recall or vice-versa. Figure 5, thus, can be used to thoroughly explore and select a robust choice of hyper-parameters (γ_1) and (γ_2) .

Although Pareto Frontier helps in choosing the best combinations of (γ_1) and (γ_2) , setting values for (γ_1) and (γ_2) that maximize precision (or recall) without ensuring some minimum recall (or precision) is not recommended as it will result in too few or too many detections, which is not practical. Thus, to avoid this, we set a minimum threshold on the F_1 score to be 0.5 in this case study. The optimal hyper-parameters achieving maximum precision, recall, and F_1 score under this condition are thus pinpointed using dominance principles in the Pareto frontier using Figure 5. Table 2 summarizes these values.

Maximizing Objective	F_1 – score	Recall	Precision	γ_1	γ_2
Precision	0.50	0.35	0.88	10	0.55
Recall	0.50	0.60	0.43	3.5	0.15
F_1 score	0.57	0.49	0.68	4.5	0.35

Table 2: Pareto Optimal (γ_1) and (γ_2) under different maximization objectives.

4.2. Comparison with Benchmark Methods

For benchmark comparisons, we utilize the COCO AP metric that has been extensively used to evaluate various state-of-art detectors on the COCO challenge [23]. This metric is based on the PASCAL VOC 2012 metric which used a similar strategy to evaluate object detectors [27]. Both VOC 2012 and COCO metrics calculate the per class Average Precision or (AP) by calculating the area under the Precision-Recall curve. This procedure is repeated for different (IoU) between 0.5 and 0.95. The individual AP for every (IoU) is reported as AP [IoU] and the mean AP is reported as AP [0.5:0.95].

Table 3 summarizes the comparisons between the results of RMOPP and other benchmarked post-processing methods. Using Table 3, it can be observed that RMOPP under different optimal settings significantly improves the COCO AP metrics for YOLOv2 without any loss in inference times (FPS). Specifically, for AP [0.5:0.95], RMOPP shows a 29% increase compared to the original benchmark of YOLOv2 [31]. Henceforth, we mainly focus on AP [0.5] because for practical applications the detected boxes must have at least a 50% intersection-over-union with the ground truth or it will be considered a bad detection. Using Table 3, it can be observed that, the proposed method easily surpasses the performance by other benchmark post-processing methods such as Soft-NMS [1] and RelationNets [17] while being significantly faster on an NVIDIA Titan X GPU. Here it should be noted that although Rank-NMS [39] achieves better performance, it is significantly slower than the proposed method. Figures 6 and 7 compares performance of YOLOv2 with traditional filtering and RMOPP. The compelling evidence in these figures helps prove the effectiveness of RMOPP over traditional algorithms.

4.3. Comparison to State-of-Art Object Detectors

Table 4 aims to compare the performance of the YOLOv2 with RMOPP to other state-of-art object detectors [14, 22, 38]. The AP [0.5] results in Table 4 show that RMOPP improves the YOLOv2 performance to become comparable to that of its slower but more complex successor- YOLOv3. It also shows that better post-processing can significantly improve the performance of single-stage detectors like YOLOv2 to match that of a two-

Method	Backbone	Post-Processing Method	FPS	γ_1	γ_2	AP [0.5 : 0.95]	AP [0.5]	AP [0.75]
YOLOv2 [31]	Darknet-19	NMS(Baseline)	40	-	-	0.216	0.440	0.192
MetanAnchorGS [42]	Darknet-19	NMS	-	-	-	0.212	0.395	-
Faster R-CNN [17]	ResNet-50	Soft-NMS	9	-	-	0.300	0.523	0.305
Faster R-CNN [17]	ResNet-50	RelationNets	17	-	-	0.303	0.519	0.315
Faster R-CNN [39]	ResNet-50-FPN	Rank-NMS	8	-	-	0.386	0.582	0.417
YOLOv2	Darknet-19	RMOPP-Best AP	40	1	0.1	0.278	0.524	0.266
YOLOv2	Darknet-19	RMOPP-Best Precision	40	10	0.55	0.216	0.366	0.229
YOLOv2	Darknet-19	RMOPP-Best Recall	40	3.5	0.15	0.268	0.502	0.258
YOLOv2	Darknet-19	RMOPP-Best F ₁ score	40	4.5	0.35	0.253	0.459	0.251

Table 3: Comparison of RMOPP across benchmarks using the COCO metrics.

Method	γ_1	γ_2	AP [0.5]
Two-Stage Detectors			
Faster R-CNN+++ [14]	-	-	0.557
Faster R-CNN w FPN [21]	-	-	0.591
Faster R-CNN w D-RMI [18]	-	-	0.555
Faster R-CNN w TDM [37]	-	-	0.577
Single-Stage Detectors			
YOLOv3 608x608 [10]	-	-	0.579
SSD513 [11]	-	-	0.504
DSSD513 [11]	-	-	0.533
RetinaNet+ResNet-101-FPN [22]	-	-	0.591
RetinaNet+ResNeXt-101-FPN [22]	-	-	0.611
CenterNet+ResNet-18 [38]	-	-	0.466
OneNet+ResNet-18 [38]	-	-	0.457
YOLOv2+RMOPP-Best AP	1	0.1	0.524
YOLOv2+RMOPP-Best Recall	3.5	0.15	0.502
YOLOv2+RMOPP-Best F ₁ score	4.5	0.35	0.459
YOLOv2+RMOPP-Best Precision	10	0.55	0.366

Table 4: Comparison of RMOPP with state-of-art.

stage detector like Faster R-CNN.

5. Conclusion and Futurework

This paper introduces RMOPP: A robust multi-objective post-processing algorithm that improves the performance of pre-trained object detectors with a negligible impact on speed. Unlike existing uni-objective post-processing methods, the proposed algorithm allows for simultaneous optimization of precision and recall in object detection pipelines. When applied to YOLOv2, RMOPP showed a 29% improvement in average precision to match similar performances of slower but more complex object detectors like YOLOv3 and Faster-RCNN. This work presents the first known usage of Pareto frontiers for post-processing hyper-parameter optimization in the field of object detec-



(a) YOLOv2 + Baseline



(b) YOLOv2 + RMOPP

Figure 6: YOLOv2+RMOPP shows significant improvement in results.

tion, to the best of our knowledge. A Bayesian post-processing technique may be feasible in future work to update the post-processing hyper-parameters for every inputted image and reduce training bias.



(a) YOLOv2 + Baseline



(b) YOLOv2 + RMOPP

Figure 7: YOLOv2+RMOPP shows significant improvement in results.

References

- [1] Navaneeth Bodla, Bharat Singh, Rama Chellappa, and Larry S Davis. Soft-NMS—improving object detection with one line of code. In *Proceedings of the IEEE international conference on computer vision*, pages 5561–5569, 2017.
- [2] Zhaowei Cai and Nuno Vasconcelos. Cascade R-CNN: Diving into High Quality Object Detection. In *Proceedings of the IEEE Computer Society Conference on Computer Vision and Pattern Recognition*, pages 6154–6162, 2018.
- [3] Nicolas Carion, Francisco Massa, Gabriel Synnaeve, Nicolas Usunier, Alexander Kirillov, and Sergey Zagoruyko. End-to-end object detection with transformers. In *European Conference on Computer Vision*, pages 213–229. Springer, 2020.
- [4] Abdallah Chehade, Scott Bonk, and Kaibo Liu. Sensory-based failure threshold estimation for remaining useful life prediction. *IEEE Transactions on Reliability*, 66(3):939–949, 2017.
- [5] Abdallah Chehade and Zunya Shi. Sensor Fusion via Statistical Hypothesis Testing for Prognosis and Degradation Analysis. *IEEE Transactions on Automation Science and Engineering*, 16(4):1774–1787, 2019.
- [6] Abdallah A Chehade and Ala A Hussein. Latent Function Decomposition for Forecasting Li-ion Battery Cells Capacity: A Multi-Output Convolved Gaussian Process Approach, 2019.

- [7] Jia Deng, Wei Dong, Richard Socher, Li-Jia Li, Kai Li, and Li Fei-Fei. ImageNet: A large-scale hierarchical image database. *2009 IEEE Conference on Computer Vision and Pattern Recognition*, pages 248–255, 2010.
- [8] Kaiwen Duan, Song Bai, Lingxi Xie, Honggang Qi, Qingming Huang, and Qi Tian. Centernet: Keypoint triplets for object detection. In *Proceedings of the IEEE/CVF International Conference on Computer Vision*, pages 6569–6578, 2019.
- [9] Kaiwen Duan, Lingxi Xie, Honggang Qi, Song Bai, Qingming Huang, and Qi Tian. Corner proposal network for anchor-free, two-stage object detection. *arXiv preprint arXiv:2007.13816*, 2020.
- [10] Ali Farhadi and Joseph Redmon. Yolov3: An incremental improvement. *Computer Vision and Pattern Recognition, cite as*, 2018.
- [11] Cheng-Yang Fu, Wei Liu, Ananth Ranga, Ambrish Tyagi, and Alexander C Berg. Dssd: Deconvolutional single shot detector. *arXiv preprint arXiv:1701.06659*, 2017.
- [12] Ross Girshick. Fast R-CNN. In *Proceedings of the IEEE International Conference on Computer Vision*, volume 2015 Inter, pages 1440–1448, 2015.
- [13] Ross Girshick, Jeff Donahue, Trevor Darrell, Jitendra Malik, U C Berkeley, and Jitendra Malik. Rich feature hierarchies for accurate object detection and semantic segmentation. In *Proceedings of the IEEE Computer Society Conference on Computer Vision and Pattern Recognition*, volume 1, page 5000, 2014.
- [14] Kaiming He, Xiangyu Zhang, Shaoqing Ren, and Jian Sun. Deep residual learning for image recognition. In *Proceedings of the IEEE conference on computer vision and pattern recognition*, pages 770–778, 2016.
- [15] Yihui He, Chenchen Zhu, Jianren Wang, Marios Savvides, and Xiangyu Zhang. Bounding box regression with uncertainty for accurate object detection. In *Proceedings of the IEEE/CVF Conference on Computer Vision and Pattern Recognition*, pages 2888–2897, 2019.
- [16] Jan Hosang, Rodrigo Benenson, and Bernt Schiele. Learning non-maximum suppression. In *Proceedings of the IEEE conference on computer vision and pattern recognition*, pages 4507–4515, 2017.
- [17] Han Hu, Jiayuan Gu, Zheng Zhang, Jifeng Dai, and Yichen Wei. Relation networks for object detection. In *Proceedings of the IEEE Conference on Computer Vision and Pattern Recognition*, pages 3588–3597, 2018.
- [18] Jonathan Huang, Vivek Rathod, Chen Sun, Menglong Zhu, Anoop Korattikara, Alireza Fathi, Ian Fischer, Zbigniew Wojna, Yang Song, Sergio Guadarrama, and Kevin Murphy. Speed/accuracy trade-offs for modern convolutional object detectors. In *Proceedings - 30th IEEE Conference on Computer Vision and Pattern Recognition, CVPR 2017*, volume 2017-Janua, pages 3296–3305, 2017.
- [19] Gandhinathan Karuppusami and R Gandhinathan. Pareto analysis of critical success factors of total quality management. *The TQM magazine*, 2006.

- [20] Hei Law and Jia Deng. Cornernet: Detecting objects as paired keypoints. In *Proceedings of the European conference on computer vision (ECCV)*, pages 734–750, 2018.
- [21] Tsung-Yi Lin, Piotr Dollár, Ross Girshick, Kaiming He, Bharath Hariharan, and Serge Belongie. Feature pyramid networks for object detection. In *Proceedings of the IEEE conference on computer vision and pattern recognition*, pages 2117–2125, 2017.
- [22] Tsung Yi Lin, Priya Goyal, Ross Girshick, Kaiming He, and Piotr Dollár. Focal Loss for Dense Object Detection. *IEEE Transactions on Pattern Analysis and Machine Intelligence*, 42(2):318–327, 2020.
- [23] Tsung Yi Lin, Michael Maire, Serge Belongie, James Hays, Pietro Perona, Deva Ramanan, Piotr Dollár, and C. Lawrence Zitnick. Microsoft COCO: Common objects in context. In *Lecture Notes in Computer Science (including subseries Lecture Notes in Artificial Intelligence and Lecture Notes in Bioinformatics)*, volume 8693 LNCS, pages 740–755, 2014.
- [24] Li Liu, Wanli Ouyang, Xiaogang Wang, Paul Fieguth, Jie Chen, Xinwang Liu, and Matti Pietikäinen. Deep Learning for Generic Object Detection: A Survey. *International Journal of Computer Vision*, 2019.
- [25] Shu Liu, Lu Qi, Haifang Qin, Jianping Shi, and Jiaya Jia. Path Aggregation Network for Instance Segmentation. *Proceedings of the IEEE Computer Society Conference on Computer Vision and Pattern Recognition*, pages 8759–8768, 2018.
- [26] Wei Liu, Dragomir Anguelov, Dumitru Erhan, Christian Szegedy, Scott Reed, Cheng Yang Fu, and Alexander C. Berg. SSD: Single shot multibox detector. *Lecture Notes in Computer Science (including subseries Lecture Notes in Artificial Intelligence and Lecture Notes in Bioinformatics)*, 9905 LNCS:21–37, 2016.
- [27] Everingham M., Van-Gool L., Williams C K I., Winn J., and Zisserman A. The Pascal Visual Object Classes (VOC) Challenge. *International Journal of Computer Vision*, 88(2):303–338, 2010.
- [28] Jiangmiao Pang, Kai Chen, Jianping Shi, Huajun Feng, Wanli Ouyang, and Dahua Lin. Libra r-cnn: Towards balanced learning for object detection. In *Proceedings of the IEEE/CVF Conference on Computer Vision and Pattern Recognition*, pages 821–830, 2019.
- [29] Steven Puttemans, Timothy Callemein, and Toon Goedeme. Building robust industrial applicable object detection models using transfer learning and single pass deep learning architectures. In *VISIGRAPP 2018 - Proceedings of the 13th International Joint Conference on Computer Vision, Imaging and Computer Graphics Theory and Applications*, volume 5, pages 209–217, 2018.
- [30] Joseph Redmon, Santosh Divvala, Ross Girshick, and Ali Farhadi. You only look once: Unified, real-time object detection. In *Proceedings of the IEEE Computer Society Conference on Computer Vision and Pattern Recognition*, volume 2016-Decem, pages 779–788, 2016.
- [31] Joseph Redmon and Ali Farhadi. YOLO9000: Better, faster, stronger. In *Proceedings - 30th IEEE Conference on Computer Vision and Pattern Recognition, CVPR 2017*, volume 2017-Janua, pages 6517–6525, 2017.
- [32] Shaoqing Ren, Kaiming He, Ross Girshick, and Jian Sun. Faster R-CNN: towards real-time object detection with region proposal networks. *IEEE transactions on pattern analysis and machine intelligence*, 39(6):1137–1149, 2016.
- [33] Mayuresh Savargaonkar and Abdallah Chehade. An Adaptive Deep Neural Network with Transfer Learning for State-of-Charge Estimations of Battery Cells. In *2020 IEEE Transportation Electrification Conference & Expo (ITEC)*, pages 598–602. IEEE, 2020.
- [34] Pierre Sermanet, David Eigen, Xiang Zhang, Michael Mathieu, Rob Fergus, and Yann LeCun. Overfeat: Integrated recognition, localization and detection using convolutional networks. In *2nd International Conference on Learning Representations, ICLR 2014 - Conference Track Proceedings*, 2014.
- [35] Zunya Shi and Abdallah Chehade. A dual-LSTM framework combining change point detection and remaining useful life prediction. *Reliability Engineering & System Safety*, 205:107257, 2021.
- [36] Zunya Shi, Mayuresh Savargaonkar, Abdallah A Chehade, and Ala A Hussein. A Long Short-Term Memory Network for Online State-of-Charge Estimation of Li-ion Battery Cells. In *2020 IEEE Transportation Electrification Conference & Expo (ITEC)*, pages 594–597. IEEE, 2020.
- [37] Abhinav Shrivastava, Rahul Sukthankar, Jitendra Malik, and Abhinav Gupta. Beyond skip connections: Top-down modulation for object detection. *arXiv preprint arXiv:1612.06851*, 2016.
- [38] Peize Sun, Yi Jiang, Enze Xie, Zehuan Yuan, Changhu Wang, and Ping Luo. OneNet: Towards End-to-End One-Stage Object Detection. *arXiv preprint arXiv:2012.05780*, 2020.
- [39] Zhiyu Tan, Xuecheng Nie, Qi Qian, Nan Li, and Hao Li. Learning to rank proposals for object detection. In *Proceedings of the IEEE/CVF International Conference on Computer Vision*, pages 8273–8281, 2019.
- [40] Yunong Tian, Guodong Yang, Zhe Wang, Hao Wang, En Li, and Zize Liang. Apple detection during different growth stages in orchards using the improved YOLO-V3 model. *Computers and Electronics in Agriculture*, 157(January):417–426, 2019.
- [41] Lachlan Tychsen-Smith and Lars Petersson. Improving object localization with fitness nms and bounded iou loss. In *Proceedings of the IEEE conference on computer vision and pattern recognition*, pages 6877–6885, 2018.
- [42] Tong Yang, Xiangyu Zhang, Zeming Li, Wenqiang Zhang, and Jian Sun. Metaanchor: Learning to detect objects with customized anchors. *Advances in Neural Information Processing Systems*, 2018-Decem:320–330, 2018.
- [43] Shifeng Zhang, Cheng Chi, Yongqiang Yao, Zhen Lei, and Stan Z Li. Bridging the gap between anchor-based and anchor-free detection via adaptive training sample selection. In *Proceedings of the IEEE/CVF Conference on Computer Vision and Pattern Recognition*, pages 9759–9768, 2020.